

Article

Thermal Conductivity of Polybutadiene Rubber from Molecular Dynamics Simulations and Measurements by the Heat Flow Meter Method

Aleksandr Vasilev ^{1,*}, Tommy Lorenz ¹, Vikram G Kamble ², Sven Wießner ² and Cornelia Breitkopf ¹

¹ Chair of Technical Thermodynamics, Technische Universität Dresden, 01069 Dresden, Germany; tommy.lorenz@tu-dresden.de (T.L.); cornelia.breitkopf@tu-dresden.de (C.B.)

² Leibniz-Institut für Polymerforschung Dresden e.V., Hohe Str. 6, 01069 Dresden, Germany; kamble@ipfdd.de (V.G.K.); wiessner@ipfdd.de (S.W.)

* Correspondence: aleksandr.vasilev@tu-dresden.de

Abstract: Thermal conductivities of polybutadiene rubbers crosslinked by 2.4 and 2.8 phr of sulfur have been found to be functions of temperature via molecular dynamics (MD) simulations using the Green–Kubo method. From an analysis of the heat flux autocorrelation functions, it has been revealed that the dominant means of heat transport in rubbers is governed by deformations of polymeric chains. Thermal conductivities of rubber samples vulcanized by 2.4 and 2.8 phr of sulfur have been measured by the heat flow meter method between 0 °C and 60 °C at atmospheric pressure. The temperature dependencies of the thermal conductivities of rubbers and their glass transition temperatures derived from MD simulations are in good agreement with the literature and experimental data. Details are discussed in the paper.



Citation: Vasilev, A.; Lorenz, T.; Kamble, V.G.; Wießner, S.; Breitkopf, C. Thermal Conductivity of Polybutadiene Rubber from Molecular Dynamics Simulations and Measurements by the Heat Flow Meter Method. *Materials* **2021**, *14*, 7737. <https://doi.org/10.3390/ma14247737>

Academic Editor: Gabriele Milani

Received: 29 October 2021

Accepted: 8 December 2021

Published: 15 December 2021

Publisher's Note: MDPI stays neutral with regard to jurisdictional claims in published maps and institutional affiliations.



Copyright: © 2021 by the authors. Licensee MDPI, Basel, Switzerland. This article is an open access article distributed under the terms and conditions of the Creative Commons Attribution (CC BY) license (<https://creativecommons.org/licenses/by/4.0/>).

Keywords: molecular dynamics simulations; force field; rubber; polybutadiene; thermal conductivity; heat flow meter method

1. Introduction

Rubbers are widely used for the development of new composite materials [1,2]. To predict the behaviour of composites under different conditions, modelings are conducted using the finite element method (FEM) [3,4]. Conservative equations are solved by FEM for each composite element. These equations require knowledge of material properties, for instance, thermal conductivity.

Knowledge of the thermal conductivity is important not only for the modeling of rubber-based composites, but also for enhancement of rubber injection molding processes [5]. The thermal conductivity of rubber can be determined by theoretical approaches and experimental techniques.

The transient hot wire method is widely used for measurements of thermal conductivities of rubbers and rubber composites [6–8]. The method is based on measuring the temperature change at some distance from the wire, which acts as a heat source and is embedded into a sample. The sample has to be isotropic. This method is faster than steady state techniques and it is an absolute method. There are standards for measurements, such as ASTM C 1113, ISO 8894-1 and ISO 8894-2.

Another transient method for measurements of thermal conductivities of rubbers and composites is the Laser Flash technique [5,9–14]. In this method the thermal diffusivity of a sample is measured, therefore it requires knowledge of heat capacity and density to find the thermal conductivity.

For materials with low thermal conductivity, such as rubber, the guarded hot plate [8,15–17] and heat flow meter methods [5,18,19] are often used. These techniques belongs to steady state approaches, as a result, require more time for measurements in com-

parison with transient methods. The guarded hot plate method is an absolute technique of measurement and is more accurate for insulators than the Laser Flash technique.

In Ref. [5] thermal conductivities of industrial rubber compounds obtained via the Guarded Heat Flow Meter, Laser Flash, Plane-Source and Line-Source techniques have been compared. The Guarded Heat Flow Meter and the Laser Flash techniques provide comparable results. It was revealed, that thermal conductivity of unfilled natural rubber remains almost constant from 60 °C until 180 °C.

In other research [20] it was observed that the thermal conductivity of rubbers varies slightly with temperature, reaches a global maximum at the glass transition temperature and then decreases. On the other hand, for some rubbers, such as natural rubber, polyisobutylene, soft and hard rubber at temperatures above room temperature, it remains almost constant [5,20,21]. More investigations are needed on the thermal conductivity's dependence on the temperature.

MD simulations can be an alternative tool for determination of the thermal conductivity as function of temperature. For instance, thermal conductivities of untreated polyisoprene and polybutadiene, obtained via MD simulations and measurements by the transient hot wire method, have been compared in Ref. [22]. The results from the simulations are in good agreement with the experimental data. The effect of the composition ratio of styrene on the thermal conductivity of butadiene styrene rubber has been found [23]. In Ref. [24], this has been calculated for soft and hard rubbers, but the difference between the results from simulations and experiments was roughly twice this. There is a great need to develop and test force fields for the prediction of the thermal conductivities of rubbers.

The study intends to compare samples, which have been exclusively prepared using experimental and theoretical methods. Special attention was paid to a detailed crosslinking of the polymers.

2. Simulation and Experimental Details

In the first part of the section, simulation details are explained and, in the second part, preparation details are given.

2.1. Simulation Details and Description of the Experimental Setup for Measurement of the Thermal Conductivity

Polybutadiene chains for the modeling of rubbers crosslinked by 2.4 and 2.8 phr (parts per hundred rubber) of sulfur have been constructed by Moltemplate software [25]. The chains consisted of 212 and 200 monomer units. A united atom force field description was used, where CH, CH₂, and CH₃ groups were modeled as one united atom; thus, carbon and hydrogen atoms have not explicitly been treated. The type of crosslink bridge considered in the research was the same as in Refs. [24,26]. The total potential energy of a polymeric system is calculated as

$$E = E_{\text{bond}} + E_{\text{angle}} + E_{\text{dihedral}} + E_{\text{non-bonded}}. \quad (1)$$

For MD simulations of the rubbers, the same force field as in Ref. [26] was used, where intra-molecular interactions are described by harmonic potentials

$$E_{\text{bond}} = \frac{K_{\text{bond}}}{2} (r - r_0)^2 \quad (2)$$

$$E_{\text{angle}} = \frac{K_{\text{angle}}}{2} (\theta - \theta_0)^2 \quad (3)$$

$$E_{\text{dihedral}} = \sum_{j=1}^3 \left(\frac{K_{\text{dihedral}j}}{2} [1 + (-1)^{j+1} \cos j\phi] \right) \quad (4)$$

where K_{bond} , K_{angle} and K_{dihedral} are force constants for bond, angle and dihedral interactions, respectively; r and r_0 are the bond length and the equilibrium bond length,

respectively; r and r_0 are the bond length and the equilibrium bond length, respectively; θ and θ_0 are the angle and equilibrium angle, respectively; ϕ is the dihedral angle.

The inter-molecular interactions were only presented by van der Waals forces, because CH, CH₂, and CH₃ groups have a total charge of zero; therefore, Coulomb interactions were not included in the mathematical model. The van der Waals forces were described by the Lennard–Jones potential, which is given by

$$E_{LJ} = \begin{cases} 4\epsilon[(\frac{\sigma}{r})^{12} - (\frac{\sigma}{r})^6] & \text{if } r \leq r_c, \\ 0 & \text{otherwise.} \end{cases} \quad (5)$$

where ϵ is the potential energy well depth, σ is the distance between particles, when the Lennard–Jones potential for the particles is equal to zero and r_c is a cutoff distance, which was equal to 10 Å in all simulations. The Lorentz–Berthelot mixing rules were used to find the missing parameters of the Lennard–Jones potential for the description of van der Waals forces between atoms of a different type. All simulations were carried out using the LAMMPS [27] software package.

Firstly, polymeric chains were randomly distributed in a periodic supercell (see Figure 1a). After that, they were crosslinked in a *NVT* ensemble using a similar algorithm to that of Ref. [28]. Then, high pressure (1000 atm) and temperature (900 K) were slowly, coolly applied to the obtained model of crosslinked chains until normal conditions were reached. This procedure was repeated several times until the density of the model reached a density close to the experimental density. Then, the system was modeled in an *NPT* ensemble for 100 ps with a time step 1 fs to equilibrate its density. In the next step, it was simulated 100 ps with the time step 1 fs in a *NVT* ensemble for equilibration of energy and temperature. Finally, when the system was placed in thermal equilibrium in an *NVE* ensemble, for every 3 ns with a time step 1 fs, the thermal conductivity of the system was calculated via the Green–Kubo formula for every correlation time interval, which was equal to 3 ps. For determination of the thermal conductivity, results from the last 50 correlation time intervals were used to find the mean value. According to the Green–Kubo formula, the thermal conductivity of isotropic material can be found as follows:

$$\lambda = \frac{V}{3k_B T^2} \int_0^\infty \langle \vec{J}(0)\vec{J}(t) \rangle dt, \quad (6)$$

where \vec{J} is the heat flux calculated by the following equation taken from Ref. [29]:

$$\vec{J} = \frac{1}{V} [\sum_i e_i \vec{v} - \sum_i S_i \vec{v}], \quad (7)$$

where e_i is the total energy of the i -th atom. The first term is the convective part of the total heat flux, which represents the heat flux due to the movement of atoms in the system. S_i is the per-atom stress tensor calculated by the equation [30]:

$$S_{ab} = -m v_a v_b - W_{ab}, \quad (8)$$

where a and b take on the values x , y , and z , and W_{ab} is the virial contribution, calculated as [30]:

$$W_{ab} = \sum_{n=1}^{N_p} r_{I0_a} F_{I_b} + \sum_{n=1}^{N_b} r_{I0_a} F_{I_b} + \sum_{n=1}^{N_a} r_{I0_a} F_{I_b} + \sum_{n=1}^{N_d} r_{I0_a} F_{I_b} + \sum_{n=1}^{N_i} r_{I0_a} F_{I_b}, \quad (9)$$

where N_p is the number of neighbors of atom I that act on atom I via van der Waals interaction, and N_b , N_a , N_d , and N_i are the numbers of bonds, angles, dihedrals, and impropers, respectively, and the atom I is included in these interactions. F_I is the force acting on atom I due to these interactions, and r_{I0} is the relative position of the atom I with respect to the geometric center of the interacting atoms.

Due to the discretization of time in MD simulations, Equation (7) can be written as follows [31]:

$$\lambda(\tau_M) = \frac{V\Delta t}{3k_B T^2} \sum_{m=1}^M \frac{1}{(N-m)} \sum_{n=1}^{N-m} J_i(n)J_j(m+n), \quad (10)$$

where $\lambda(\tau_M)$ is the thermal conductivity obtained from summation to time step M ($M = 0, 1, \dots, N-1$), N is the total number of simulation steps, and $\tau_M = M\Delta t$.

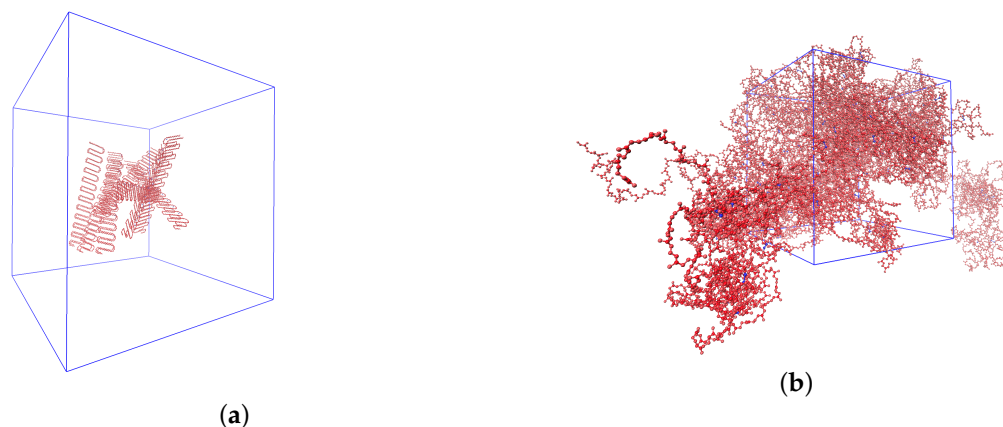


Figure 1. (a) Randomly distributed 16 polybutadiene chains in the periodic supercell (size of the cell is $440 \text{ \AA} \times 440 \text{ \AA} \times 440 \text{ \AA}$); (b) model of polybutadiene rubber vulcanized by 2.8 phr of sulfur in the periodic supercell (size of the cell is $69 \text{ \AA} \times 69 \text{ \AA} \times 69 \text{ \AA}$).

To investigate the influence of size effects on the thermal conductivity, the results for systems of untreated polybutadiene with 12,000 and 24,000 united atoms were compared. For the system with 12,000 united atoms (size of the cell $66 \text{ \AA} \times 66 \text{ \AA} \times 66 \text{ \AA}$) the thermal conductivity was equal to 0.199 W/m/K , whereas for the bigger system (24,000 united atoms, size of the cell $83 \text{ \AA} \times 83 \text{ \AA} \times 83 \text{ \AA}$) the thermal conductivity was 0.201 W/m/K . For MD simulations of rubbers crosslinked with 2.4 phr and 2.8 phr of sulfur, models with 14,352 (size of the cell $70 \text{ \AA} \times 70 \text{ \AA} \times 70 \text{ \AA}$) and 13,728 (size of the cell $69 \text{ \AA} \times 69 \text{ \AA} \times 69 \text{ \AA}$) united atoms were used (see Figure 1b), respectively.

The measurement of the thermal conductivity of rubber samples was carried out using the heat flow meter method. This approach is based on obtaining a constant heat flux and temperature gradient inside a sample. When this condition is achieved, Fourier's law of thermal conduction can be used to calculate the thermal conductivity of the sample

$$\lambda_z = -\frac{\vec{q}_z}{\frac{dT}{dz}} \quad (11)$$

where \vec{q}_z is the heat flux in z direction, which was taken as the average value of heat fluxes measured by upper- and lower-heat-flux sensors (see Figure 2a), dT is the temperature difference between hot and cold plates and dz is the distance between the plates.

Schematic description of the method is presented in Figure 2a. The sample is placed between hot and cold plates. The upper surface of the sample is heated by a foil connected to a cooper plate. Constant current and voltage were applied to maintain the temperature of the hot plate. Between the plate and the sample temperature, the heat flux sensor was established. Similarly, temperature and heat flux sensors were set up between the bottom surface of the sample and cold plate. The maximal uncertainty of the heat flux sensor was no more than 5%. The temperature of the cold plate was maintained by thermostat. The experimental set up used for measurements is shown in Figure 2b.

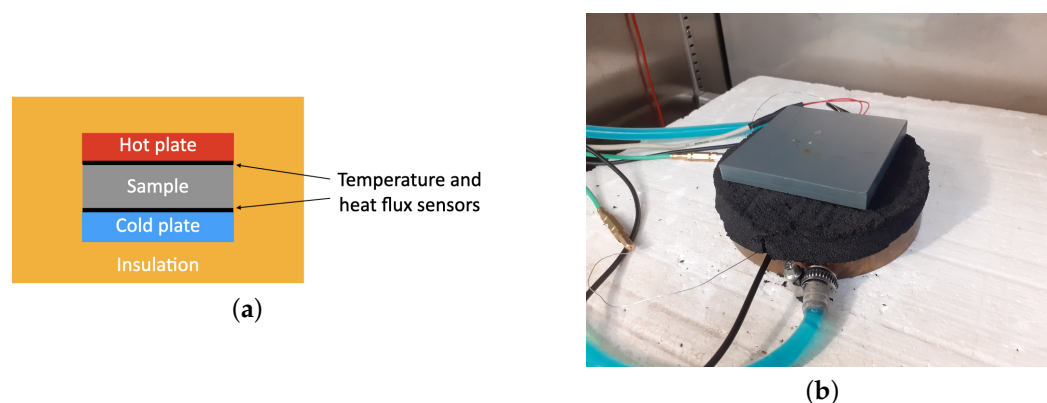


Figure 2. (a) Scheme of Heat Flow Meter method; (b) experimental setup.

2.2. Preparation of Samples for Experiments

To obtain an experimentally equivalent sample basis, new liquid polybutadiene rubber (LBR)-based elastomers were prepared (see Figure 3). A commercially available high-*cis* LBR-homopolymer (1,2-*vinyl* content below 5 mol %) with a molecular weight of 45 kDa (LBR-300 by Kuraray Europe GmbH, Hattersheim, Germany) was selected as raw polymer. The crosslinking of the rubber was based on an accelerated sulfur vulcanization system. Sulfur (purity ~99.5 %) and Zinc Oxide (purity ~99.5 %) were obtained from Acros Organics N.V. (Geel, Belgium) and used as received. A general purpose grade Stearic acid was purchased from Fisher Scientific GmbH (Schwerte, Germany). The accelerators N-cyclohexyl-2-benzothiazole sulfenamide (CBS) and Tetrabenzylthiuramdisulfide (TBzTD) were obtained from Rhein Chemie GmbH (Mannheim, Germany) and Avokal Heller GmbH (Wuppertal, Germany), respectively. To achieve two different crosslink densities of the vulcanizates, the sulfur content was varied. The formulations are shown in Table 1. All quantities refer to parts per hundred rubber (phr).

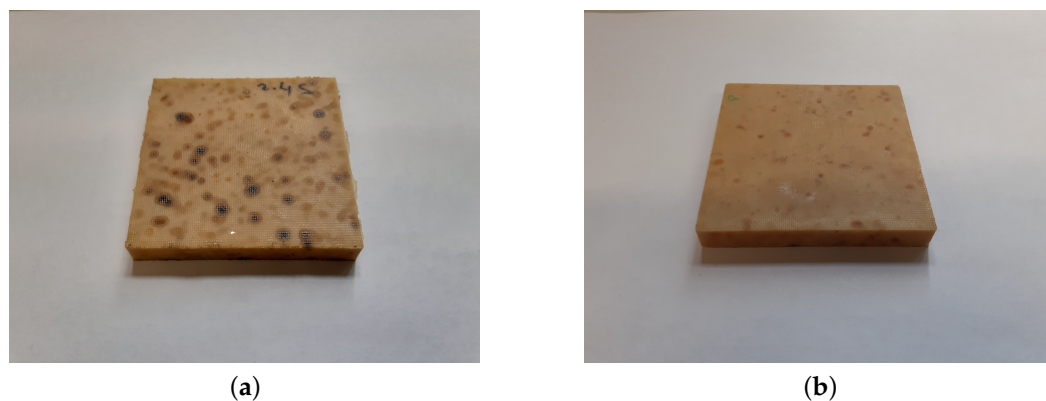


Figure 3. (a) Sample of polybutadiene rubber crosslinked by 2.4 phr of sulfur; (b) sample of polybutadiene rubber crosslinked by 2.8 phr of sulfur.

Table 1. Rubber and chemicals used to prepare samples.

Ingredient	Quantity (phr)
Liquid butadiene rubber (LBR)	100
Zinc Oxide	3
Stearic acid	2
TBzTD	1
CBS	1.5
Sulfur	2.4 and 2.8

The compositions shown in Table 1 were mixed in a scale of 50 g at a temperature of 25 °C using a liquid mixer working with the dual asymmetric centrifuge principal

(SpeedMixer, DAC150 SP by Hauschild GmbH & Co KG, Hamm, Germany) at a defined mixing sequence as follows: 800 rpm (5 s), 2500 rpm (120 s), 1200 rpm (5 s), 2500 rpm (100 s), 800 rpm (5 s) and this cycle was repeated three times to ensure the homogeneity of the mixture. Then, the formulations were transferred to a metal mold with rectangular cavities (50 mm × 50 mm × 10 mm and 100 mm × 100 mm × 2 mm) and allowed to cure to their respective T90 time in a compression molding machine (Model TP1000 by Fontijne Presses B.V., Delft, The Netherlands) at a temperature of 150 °C and a force of 150 kN.

3. Results and Discussion

The dynamic mechanical behavior of rectangular samples (30 mm × 10 mm × 2 mm) was characterized by temperature sweep experiments using a mechanical spectrometer (GABO EPLEXOR 150N, GABO QUALIMETER Testanlagen GmbH, Ahlstedt, Germany) in tension mode at 0.5 % dynamic strain amplitude, 2 K/min heating rate (temperature range of −120 °C to 100 °C) and 10 Hz frequency. The storage modulus (E') and mechanical loss factor ($\tan\delta$) are shown in Figure 4.

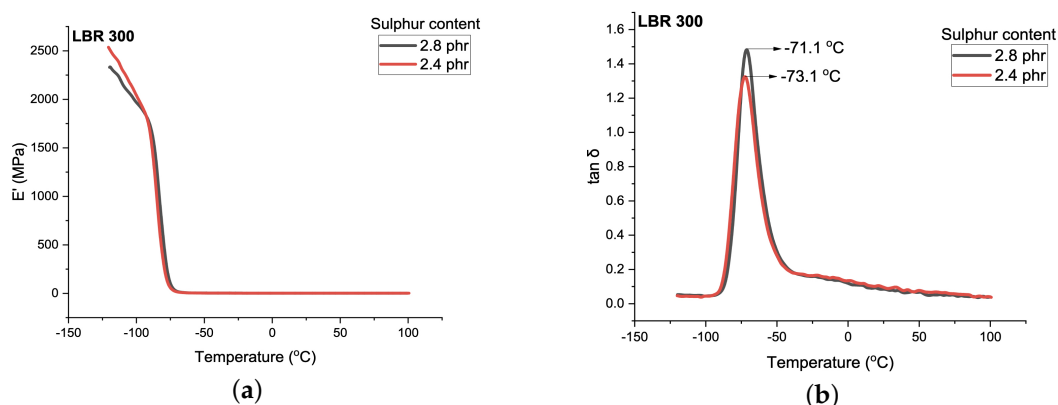


Figure 4. (a) Storage modulus (E'); (b) mechanical loss factor ($\tan\delta$) as a function of temperature.

From the local maximum of the mechanical loss factor (see Figure 4) the glass transition temperatures $T_{g, DMA}$ can be estimated with ~ -71 °C . . . -73 °C, indicating a slight shift in $T_{g, DMA}$ towards higher temperatures at an increasing degree of crosslinking, as already known from the literature [32]. This is in agreement with the published data on the glass transition temperature of polybutadiene rubbers with a different microstructure [33]. In this context, it must be noted that the glass transition temperatures obtained by dynamic scanning calorimetry (DSC) are usually ~ 20 K lower than those obtained from DMA method [34].

Heat fluxes through the upper and lower surfaces of the sample of polybutadiene rubber vulcanized by 2.4 phr of sulfur are presented in Figure 5a. For calculation of the thermal conductivity, only datapoints from steady-state regime were taken. The heat fluxes in the steady-state regime are presented in Figure 5b.

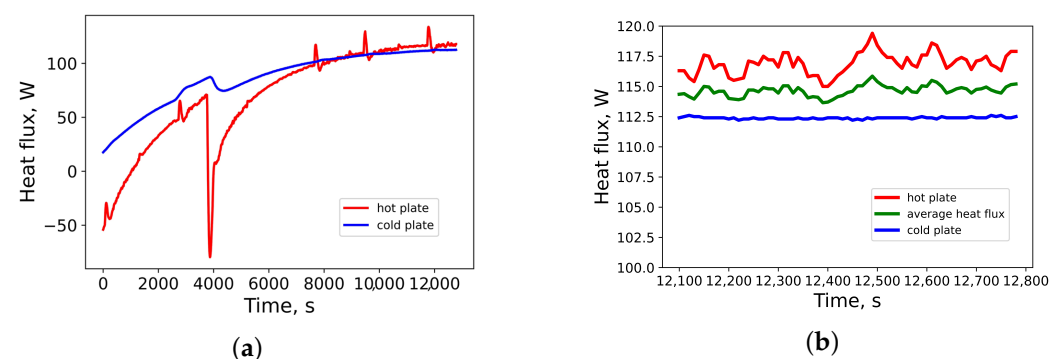


Figure 5. (a) Heat fluxes through hot and cold plates ; (b) heat fluxes in steady-state regime.

The thermal conductivity of polybutadiene rubber crosslinked by 2.4 phr of sulfur as function of temperature is shown in Figure 6. Standard deviation of results from MD simulations is below 3 %, whereas the deviation of measurements is 6 %. From Figure 6(a), that thermal conductivity increases until around $-50\text{ }^{\circ}\text{C}$ degrees and, above this temperature, it decreases until it reaches room temperature. This means that the glass transition temperature of the rubber is close to $-50\text{ }^{\circ}\text{C}$ degrees, which is in good agreement with the data from measurements (see Figure 4). At temperatures above room temperature, the thermal conductivity slightly decreases. This is in agreement with the results from Ref. [20].

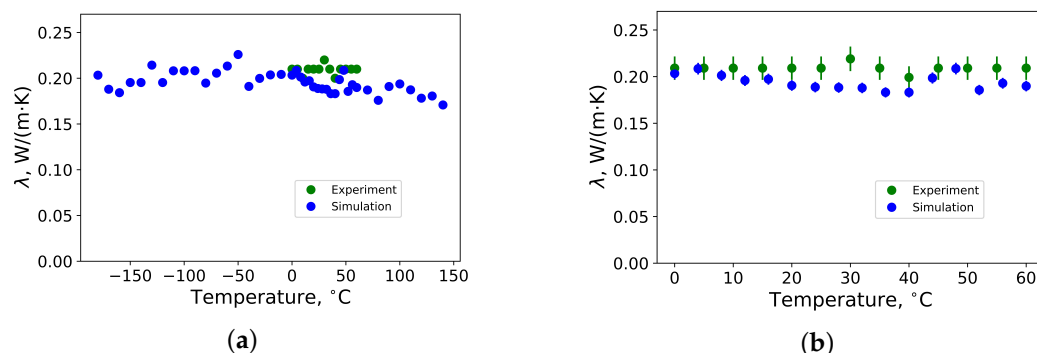


Figure 6. (a) Thermal conductivity of polybutadiene rubber vulcanized by 2.4 phr of sulfur in temperature range between $-180\text{ }^{\circ}\text{C}$ and $140\text{ }^{\circ}\text{C}$ from MD simulations; (b) thermal conductivity of polybutadiene rubber vulcanized by 2.4 phr of sulfur in temperature range between $0\text{ }^{\circ}\text{C}$ and $60\text{ }^{\circ}\text{C}$ from MD simulations (blue) and measurements (green) by the Heat Flow Meter method.

For the sample of polybutadiene rubber crosslinked by 2.8 phr of sulfur, the same tendency is observed, where thermal conductivity above room temperature remains almost constant or slightly decreases (see Figure 7). It has a global maximum of approximately $-50\text{ }^{\circ}\text{C}$ degrees, which is also close to the experimental value (see Figure 4).

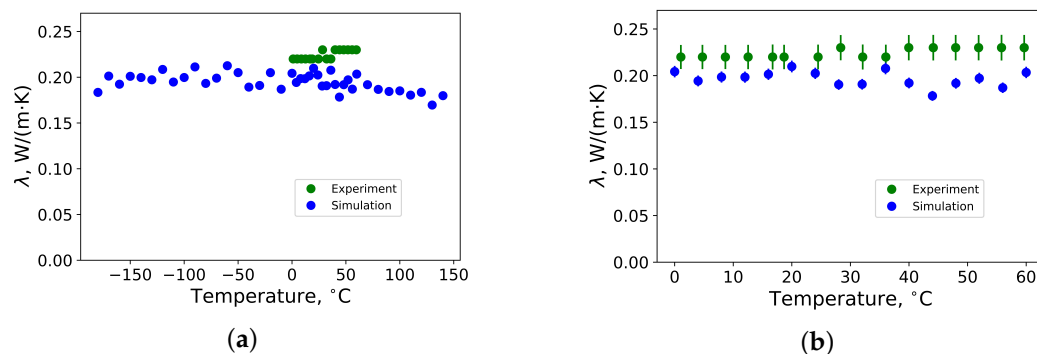


Figure 7. (a) Thermal conductivity of polybutadiene rubber vulcanized by 2.8 phr of sulfur in temperature range between $-180\text{ }^{\circ}\text{C}$ and $140\text{ }^{\circ}\text{C}$ from MD simulations; (b) thermal conductivity of polybutadiene rubber vulcanized by 2.8 phr of sulfur in temperature range between $0\text{ }^{\circ}\text{C}$ and $60\text{ }^{\circ}\text{C}$ from MD simulations (blue) and measurements (green) by the Heat Flow Meter method.

In Ref. [24], a simple harmonic oscillator model has been proposed for the estimation of the frequency of phonon modes, which are dominant in heat transfer. According to the model, the first minima of the heat flux autocorrelation functions are connected with the frequency of these modes. Applying this result to the normalized heat flux autocorrelation functions (NHFACF) of rubbers (see Figure 8a), one can see that the first minimum of NHFACF is located roughly at 15 fs, which corresponds to wave number of $\bar{\nu} \approx 353\text{ cm}^{-1}$. This is close to the wave number of C-C-C deformations [35]. As a result, the dominant means of heat transport in rubber is governed by deformations of

polymeric chains. A similar heat transport mechanism was observed in polyethylene and polyisoprene rubbers [24,36].

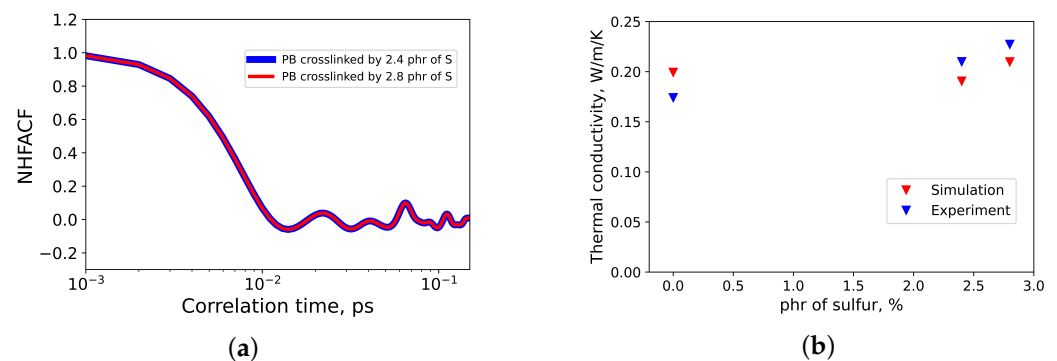


Figure 8. (a) The first minima of normalized heat flux autocorrelation functions (NHFAF) of polybutadiene crosslinked by 2.4 and 2.8 phr of sulfur; (b) thermal conductivities of polybutadiene rubbers crosslinked by different amounts of sulfur.

Combining this with the results taken from Refs. [22,26], it was revealed that the thermal conductivity of polybutadiene rubber increases with an increase in sulfur content (see Figure 8b). The same tendency was observed in experiments [37] and in MD simulations of polyisoprene and polybutadiene rubbers [26].

4. Conclusions

The thermal conductivities of polybutadiene rubbers vulcanized by 2.4 and 2.8 phr of sulfur were calculated by MD simulations and measured by the heat flow meter method in the temperature range from 0 °C to 60 °C at atmospheric pressure. Results from MD simulations are in good agreement with experimental data. From an analysis of the normalized heat flux autocorrelation function, it was found that the main mechanism of heat transfer in these rubbers is caused by the transport of low-frequency phonons, which are caused by deformations of polymeric chains. The tested force field is sufficient for the prediction of thermal conductivities of polybutadiene rubbers and, for an estimation, their glass transition temperatures. Finally, it can be concluded that MD simulations using the Green–Kubo approach can be used to determine the thermal conductivities of rubbers as a function of temperature for their macro-scale modeling by FEM.

Author Contributions: Conceptualization, A.V.; software, A.V.; data curation, A.V. (MD and hot plate) and V.G.K. (polymer synthesis and modulus); formal analysis, A.V. (MD and hot plate) and V.G.K. (polymer synthesis and modulus); investigation, A.V. (MD and hot plate) and V.G.K. (polymer synthesis and modulus); methodology, A.V. (MD and hot plate) and V.G.K. (polymer synthesis and modulus); resources, V.G.K. and T.L.; validation, A.V. (MD and hot plate) and V.G.K. (polymer synthesis and modulus); visualization, A.V.; writing—original draft, A.V. (MD and hot plate) and V.G.K. (polymer synthesis and modulus); writing—review and editing, T.L., S.W. and C.B.; supervision, T.L., S.W. and C.B.; project administration, C.B. All authors have read and agreed to the published version of the manuscript.

Funding: The DFG research project 380321452/GRK2430 was supported by the Deutsche Forschungsgemeinschaft (DFG, German Research Foundation). The financial support is gratefully acknowledged.

Institutional Review Board Statement: Not applicable.

Informed Consent Statement: Not applicable.

Data Availability Statement: Not applicable.

Acknowledgments: The authors thank Sebastian Pinnau and Julian Volland for the help with measurements by the Heat Flow Meter method. The computational time and support by the Zentrum für

Informationsdienste und Hochleistungsrechnen (ZIH) in Dresden are highly appreciated (project p_thermo_dat).

Conflicts of Interest: The authors declare no conflict of interest.

Abbreviations

The following abbreviations are used in this manuscript:

FEM (finite element method), phr (parts per hundred rubber), *NPT* (isothermal–isobaric ensemble), *NVT* (canonical ensemble), *NVE* (microcanonical ensemble), DSC (dynamic scanning calorimetry), DMA (dynamic strain amplitude), NHFACF (normalized heat flux autocorrelation function).

References

1. Sienkiewicz, M.; Janik, H.; Borzędowska-Labuda, K.; Kucińska-Lipka, J. Environmentally friendly polymer-rubber composites obtained from waste tyres: A review. *J. Clean. Prod.* **2017**, *147*, 560–571. [[CrossRef](#)]
2. Stelescu, M.D.; Manaila, E.; Craciun, G.; Dumitrascu, M. New green polymeric composites based on hemp and natural rubber processed by electron beam irradiation. *Sci. World J.* **2014**, *2014*, 684047. [[CrossRef](#)]
3. Gracia, L.; Liarte, E.; Pelegay, J.; Calvo, B. Finite element simulation of the hysteretic behaviour of an industrial rubber. Application to design of rubber components. *Finite Elem. Anal. Des.* **2010**, *46*, 357–368. [[CrossRef](#)]
4. Cugliari, J. Investigation of Contact Mechanics and Friction of Rubber Compounds by Experimental Techniques and Numerical Simulations. Ph.D. Thesis, Institutionelles Repositorium der Leibniz Universität Hannover, Hannover, Germany, 2021.
5. Kerschbaumer, R.C.; Stieger, S.; Gschwandl, M.; Hutterer, T.; Fasching, M.; Lechner, B.; Meinhart, L.; Hildenbrandt, J.; Schrittmesser, B.; Fuchs, P.F.; et al. Comparison of steady-state and transient thermal conductivity testing methods using different industrial rubber compounds. *Polym. Test.* **2019**, *80*, 106121. [[CrossRef](#)]
6. Benazzouk, A.; Douzane, O.; Mezreb, K.; Laidoudi, B.; Quéneudec, M. Thermal conductivity of cement composites containing rubber waste particles: Experimental study and modelling. *Constr. Build. Mater.* **2008**, *22*, 573–579. [[CrossRef](#)]
7. Sandberg, O.; Bäckström, G. Thermal properties of natural rubber versus temperature and pressure. *J. Appl. Phys.* **1979**, *50*, 4720–4724. [[CrossRef](#)]
8. Wilk, J.; Smusz, R.; Filip, R.; Chmiel, G.; Bednarczyk, T. Experimental investigations on graphene oxide/rubber composite thermal conductivity. *Sci. Rep.* **2020**, *10*, 15533. [[CrossRef](#)]
9. Tian, L.; Wang, Y.; Li, Z.; Mei, H.; Shang, Y. The thermal conductivity-dependant drag reduction mechanism of water droplets controlled by graphene/silicone rubber composites. *Exp. Therm. Fluid Sci.* **2017**, *85*, 363–369. [[CrossRef](#)]
10. Gschwandl, M.; Kerschbaumer, R.C.; Schrittmesser, B.; Fuchs, P.F.; Stieger, S.; Meinhart, L. Thermal conductivity measurement of industrial rubber compounds using laser flash analysis: Applicability, comparison and evaluation. In *AIP Conference Proceedings*; AIP Publishing LLC: Melville, NY, USA, 2019; Volume 2065, p. 030041.
11. Wang, F.; Drzal, L.T.; Qin, Y.; Huang, Z. Enhancement of fracture toughness, mechanical and thermal properties of rubber/epoxy composites by incorporation of graphene nanoplatelets. *Compos. Part A Appl. Sci. Manuf.* **2016**, *87*, 10–22. [[CrossRef](#)]
12. Song, J.; Ma, L.; He, Y.; Yan, H.; Wu, Z.; Li, W. Modified graphite filled natural rubber composites with good thermal conductivity. *Chin. J. Chem. Eng.* **2015**, *23*, 853–859. [[CrossRef](#)]
13. Song, J.p.; Tian, K.y.; Ma, L.x.; Li, W.; Yao, S.c. The effect of carbon black morphology to the thermal conductivity of natural rubber composites. *Int. J. Heat Mass Transf.* **2019**, *137*, 184–191. [[CrossRef](#)]
14. Xue, Y.; Li, X.; Wang, H.; Zhao, F.; Zhang, D.; Chen, Y. Improvement in thermal conductivity of through-plane aligned boron nitride/silicone rubber composites. *Mater. Des.* **2019**, *165*, 107580. [[CrossRef](#)]
15. Kobari, T.; Okajima, J.; Komiyama, A.; Maruyama, S. Development of guarded hot plate apparatus utilizing Peltier module for precise thermal conductivity measurement of insulation materials. *Int. J. Heat Mass Transf.* **2015**, *91*, 1157–1166. [[CrossRef](#)]
16. Yang, I.; Kim, D.; Lee, S. Construction and preliminary testing of a guarded hot plate apparatus for thermal conductivity measurements at high temperatures. *Int. J. Heat Mass Transf.* **2018**, *122*, 1343–1352. [[CrossRef](#)]
17. Headley, A.J.; Hileman, M.B.; Robbins, A.S.; Piekos, E.S.; Stirrup, E.K.; Roberts, C.C. Thermal conductivity measurements and modeling of ceramic fiber insulation materials. *Int. J. Heat Mass Transf.* **2019**, *129*, 1287–1294. [[CrossRef](#)]
18. Cha, J.; Seo, J.; Kim, S. Building materials thermal conductivity measurement and correlation with heat flow meter, laser flash analysis and TCI. *J. Therm. Anal. Calorim.* **2012**, *109*, 295–300. [[CrossRef](#)]
19. Song, J.; Li, X.; Tian, K.; Ma, L.; Li, W.; Yao, S. Thermal conductivity of natural rubber nanocomposites with hybrid fillers. *Chin. J. Chem. Eng.* **2019**, *27*, 928–934. [[CrossRef](#)]
20. Eiermann, K.; Hellwege, K.X. Thermal conductivity of high polymers from -180°C to 90°C . *J. Polym. Sci.* **1962**, *57*, 99–106. [[CrossRef](#)]
21. Carwile, L.C.; Hoge, H.J. Thermal conductivity of soft vulcanized natural rubber, selected values. *Rubber Chem. Technol.* **1966**, *39*, 126–131. [[CrossRef](#)]
22. Vasilev, A.; Lorenz, T.; Breikopf, C. Thermal conductivity of polyisoprene and polybutadiene from molecular dynamics simulations and transient measurements. *Polymers* **2020**, *12*, 1081. [[CrossRef](#)] [[PubMed](#)]

23. Zhao, X.; Fu, B.; Zhang, W.; Li, H.; Lu, Y.; Gao, Y.; Zhang, L. Increasing the thermal conductivity of styrene butadiene rubber: insights from molecular dynamics simulation. *RSC Adv.* **2020**, *10*, 23394–23402. [[CrossRef](#)]
24. Engelmann, S.; Meyer, J.; Hentschke, R. Computer simulation of thermal conductivity in vulcanized polyisoprene at variable strain and temperature. *Phys. Rev. B* **2017**, *96*, 054110. [[CrossRef](#)]
25. Jewett, A.I.; Zhuang, Z.; Shea, J.E. Moltemplate a coarse-grained model assembly tool. *Biophys. J.* **2013**, *104*, 169. [[CrossRef](#)]
26. Vasilev, A.; Lorenz, T.; Breitkopf, C. Thermal Conductivities of Crosslinked Polyisoprene and Polybutadiene from Molecular Dynamics Simulations. *Polymers* **2021**, *13*, 315. [[CrossRef](#)]
27. Plimpton, S. Fast parallel algorithms for short-range molecular dynamics. *J. Comput. Phys.* **1995**, *117*, 1–19. [[CrossRef](#)]
28. Hager, J.; Hentschke, R.; Hojdis, N.W.; Karimi-Varzaneh, H.A. Computer simulation of particle–particle interaction in a model polymer nanocomposite. *Macromolecules* **2015**, *48*, 9039–9049. [[CrossRef](#)]
29. Compute Heat/Flux Command. Available online: https://docs.lammps.org/compute_heat_flux.html (accessed on 25 October 2021).
30. Compute Centroid/Stress/Atom Command. Available online: https://docs.lammps.org/compute_stress_atom.html (accessed on 20 October 2021).
31. Schelling, P.K.; Phillpot, S.R.; Keblinski, P. Comparison of atomic-level simulation methods for computing thermal conductivity. *Phys. Rev. B* **2002**, *65*, 144306. [[CrossRef](#)]
32. Bandzierz, K.; Reuvekamp, L.; Dryzek, J.; Dierkes, W.; Blume, A.; Bielinski, D. Influence of network structure on glass transition temperature of elastomers. *Materials* **2016**, *9*, 607. [[CrossRef](#)]
33. Rivera, M.R.; Nájera, R.H.; Tapia, J.J.B.; Guerrero, L.R. Structure and properties of model polybutadienes—Effect of microstructure on the dynamic mechanical properties of rubber. *J. Elastomers Plast.* **2005**, *37*, 267–278. [[CrossRef](#)]
34. Lewandowska, K.; Furtos, G. Study of apatite layer formation on SBF-treated chitosan composite thin films. *Polym. Test.* **2018**, *71*, 173–181. [[CrossRef](#)]
35. Nallasamy, P.; Anbarasan, P.; Mohan, S. Vibrational spectra and assignments of cis-and trans-1, 4-polybutadiene. *Turk. J. Chem.* **2002**, *26*, 105–112.
36. Zhao, J.; Jiang, J.W.; Wei, N.; Zhang, Y.; Rabczuk, T. Thermal conductivity dependence on chain length in amorphous polymers. *J. Appl. Phys.* **2013**, *113*, 184304. [[CrossRef](#)]
37. Cheheb, Z.; Mousseau, P.; Sarda, A.; Deterre, R. Thermal conductivity of rubber compounds versus the state of cure. *Macromol. Mater. Eng.* **2012**, *297*, 228–236. [[CrossRef](#)]